AD-A047 150 DAVID W TAYLOR NAVAL SHIP RESEARCH AND DEVELOPMENT CE--ETC F/G 20/4
THEORETICAL ASPECTS OF DROMEDARYFOIL.(U)
NOV 77 T C TAI

UNCLASSIFIED DTNSRDC-77-0104 NL

1 OF 1
ADA
047150

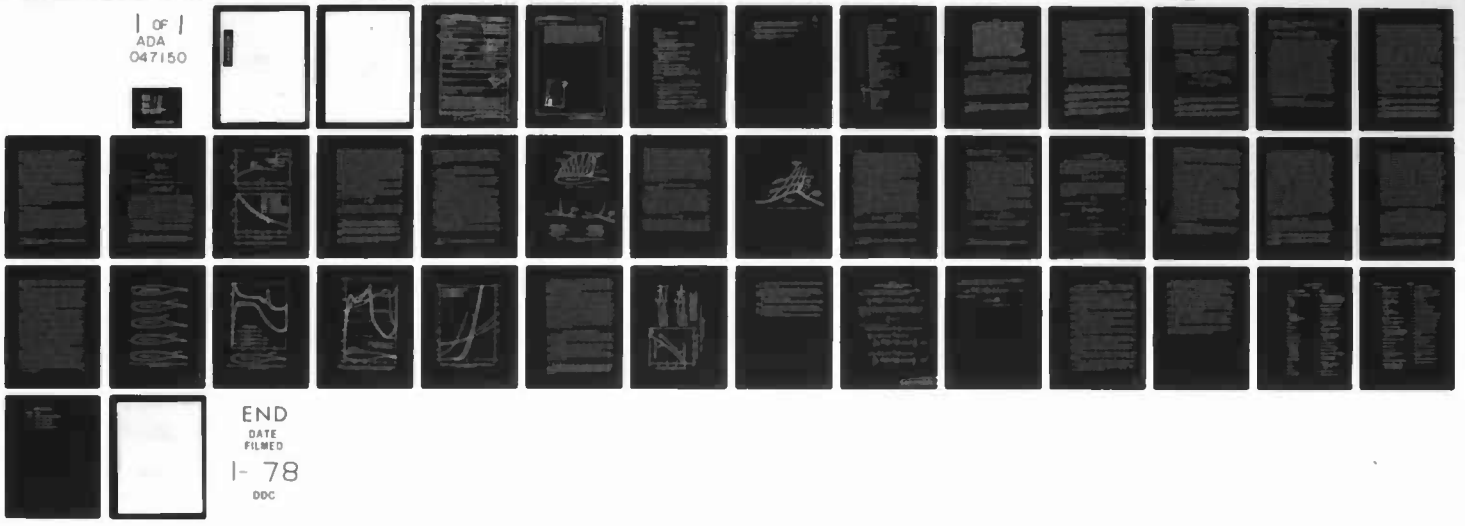

END
DATE FILMED
1-78
DDC

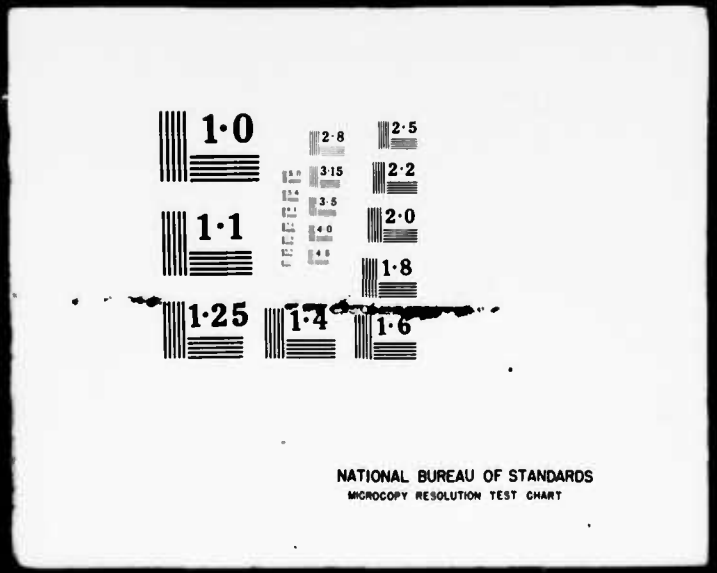

UNCLASSIFIED

SECURITY CLASSIFICATION OF THIS PAGE (When Date Entered)

REPORT DOCUMENTATION PAGE

READ INSTRUCTIONS BEFORE COMPLETING FORM

1. REPORT NUMBER: DTNSRDC-77-0104
2. GOVT ACCESSION NO.
3. RECIPIENT'S CATALOG NUMBER

4. TITLE (and Subtitle): THEORETICAL ASPECTS OF DROMEDARYFOIL.

5. TYPE OF REPORT & PERIOD COVERED: Interim Report. Jan 1976-Jan 1977

6. PERFORMING ORG. REPORT NUMBER

7. AUTHOR(s): Tsze C. Tai

8. CONTRACT OR GRANT NUMBER(s)

9. PERFORMING ORGANIZATION NAME AND ADDRESS
David W. Taylor Naval Ship Research and Development Center
Bethesda, Maryland 20084

10. PROGRAM ELEMENT, PROJECT, TASK AREA & WORK UNIT NUMBERS
Program Element 61153N
Task Area R023-02-001
Work Unit 1-1606-300

11. CONTROLLING OFFICE NAME AND ADDRESS
Naval Air Systems Command
Code AIR-320
Washington, D.C. 20361

12. REPORT DATE: November 1977

13. NUMBER OF PAGES: 40

14. MONITORING AGENCY NAME & ADDRESS (if different from Controlling Office)

15. SECURITY CLASS. (of this report): UNCLASSIFIED

15a. DECLASSIFICATION/DOWNGRADING SCHEDULE

16. DISTRIBUTION STATEMENT (of this Report)
RR023-02 RR023-02-01
APPROVED FOR PUBLIC RELEASE: DISTRIBUTION UNLIMITED

17. DISTRIBUTION STATEMENT (of the abstract entered in Block 20, if different from Report)

18. SUPPLEMENTARY NOTES

19. KEY WORDS (Continue on reverse side if necessary and identify by block number)

Transonic Flow
Oblique Shock Wave
Supercritical Airfoil
Hump

20. ABSTRACT (Continue on reverse side if necessary and identify by block number)

A new airfoil design (called a dromedaryfoil) has been developed using a single hump on a modified supercritical airfoil for limiting the center of pressure excursion and maximizing the drag divergence Mach number. Derivation of the hump is based on isentropic compression in the fore part and incipient separation in the rear. The former leads to a weakened shock wave and the latter to high pressure recovery after the shock. The shock

(Continued on reverse side)

DD FORM 1 JAN 73 1473 EDITION OF 1 NOV 65 IS OBSOLETE S/N 0102-LF-014-6601

UNCLASSIFIED

SECURITY CLASSIFICATION OF THIS PAGE (When Date Entered)

387682

(Block 20 - continued)

will theoretically locate at the peak of the hump to form a fixed pressure pattern under different flight speeds. The shock foot will be inclined at a deflection angle of the hump measured from the normal of the fore hump surface at the peak. Theoretical results indicate considerably shorter center-of-pressure travel for a dromedaryfoil than for a supercritical airfoil with equal wave drag. However, improper humping would be penalized by increased wave drag. At high supercritical flows, the shock strength would be limited by $(M_1 \sin \beta)_{max} = 1.483$. Experimental verification of theoretical predictions is planned.

TABLE OF CONTENTS

LIST OF FIGURES

NOTATION

C_D	Drag coefficient
C_L	Lift coefficient
C_m	Pitching moment coefficient
C_p	Pressure coefficient
C.P.	Center of Pressure
c	Chord of airfoil
D	Drag
G	Function as defined in Equation (3)
M	Mach number
P	Pressure
R	Gas constant
s	Entropy
V	Velocity
x,y	Cartesian coordinates
α	Angle of attack
β	Shock angle
γ	Ratio of specific heats; for air $\gamma = 1.4$
θ	Surface inclination
λ	Deflection angle of a hump
μ	Mach angle
ρ	Density
σ	Shock surface

Subscripts

0	Stagnation condition
1,2	Before and aft shock
C.P.	Center of pressure
lim	Limiting
n	Normal
w	Wave
∞	Free stream

ABSTRACT

An airfoil design (called a dromedaryfoil) has been developed using a single hump on a modified supercritical airfoil for limiting the center of pressure excursion and maximizing the drag divergence Mach number. Derivation of the hump is based on isentropic compression in the fore part and incipient separation in the rear. The former leads to a weakened shock wave and the latter to high pressure recovery after the shock. The shock will theoretically locate at the peak of the hump to form a fixed pressure pattern under different flight speeds. The shock foot will be inclined at a deflection angle of the hump measured from the normal of the fore hump surface at the peak. Theoretical results indicate considerably shorter center-of-pressure travel for a dromedaryfoil than for a supercritical airfoil with equal wave drag. However, improper humping would be penalized by increased wave drag. At high supercritical flows, the shock strength would be limited by $(M_1 \sin \beta)_{max} = 1.483$. Experimental verification of theoretical predictions is planned.

ADMINISTRATION INFORMATION

The work reported herein has been authorized and funded by the Naval Air Systems Command (AIR-320) under AIRTASK R023-02-001 and DTNSRDC Work Unit 1-1606-300, and monitored by R.F. Siewert, Jr.

INTRODUCTION

Experimental and theoretical advances in transonic aerodynamics during recent years have led to the concept of "supercritical airfoils" as a new design criterion for a wing traveling at high subsonic speeds. The "peaky" airfoil of Pearcey[1] represents the first attempt specifically designed to improve airfoil performance in a supercritical flow. Peaky velocity is generated near the leading edge to allow favorable development of the supersonic flow ahead of the shock, forming a "nose loaded" flow pattern.

---

[1]Pearcey, H.H., "The Aerodynamic Design of Section Shapes for Swept Wings," Advances in Aeronautical Sciences, Vol. 3, Pergamon Press, New York (1961), pp. 277-322. A complete listing of references is given on pages 31 and 32.

It was followed by Whitcomb[2] who designed an airfoil with the shock wave moved back considerably to the rear of the airfoil, resulting in an aft loaded flow pattern. The latter achieved a 0.1 delay in drag divergence Mach number as compared with 0.02 to 0.03 by the former. Yoshihara[3] used the peaky distribution and aft cambering to derive an airfoil with combined fore and aft loading concepts.

Theoretically, Nieuwland[4] and Korn and Garabedian[5] derived a series of "shockless" airfoils using the inviscid potential flow equations. The shock wave is eliminated by assuming isentropic flow. It is interesting to note that the theoretical airfoil of Korn and Garabedian[5] yields a profile similar to that obtained empirically by Whitcomb[2] using an entirely different approach.

Away from the design condition, the shock wave plays a dominant role for both supercritical and conventional airfoils. The state of the art, as advanced by the "supercritical airfoil" is its ability to delay the transonic drag divergence about 0.1 Mach numbers higher. Improvement in performance offered is thus fairly limited at off-design operations.

The problem of drag divergence and transonic buffeting therefore remains a severe one regardless of the type of airfoil. The question then is how to limit the drag value and reduce buffet magnitude if the aircraft operates frequently at off-design conditions such as in a military maneuver.

---

[2]Whitcomb, R.T., "Basic Results of a Wind-Tunnel Investigation of an Integral (Unslotted) Supercritical Airfoil Section," Langley Working Paper LWP-505 (Nov 1967); Declassified (Apr 1974).

[3]Yoshihara, H. et al., "Lift Augmentation on Planar Airfoils in the Transonic Regime--A High Reynolds Number Wind Tunnel Study," Convair Aerospace Division of General Dynamics, Report CASD-NSC-73-001, San Diego, Calif. (Sep 1973).

[4]Nieuwland, G.Y., "Transonic Potential Flow around a Family of Quasi-Elliptical Aerofoil Sections," National Aerospace Laboratory, Amsterdam, The Netherlands, TR T-122 (Jul 1967).

[5]Garabedian, P.R. and D.G. Korn, "Numerical Design of Transonic Airfoils," Numerical Solution of Partial Differential Equations, Vol. 2, Academic Press, New York (1971), pp. 253-271.

Experience in analyzing flows[6] and in using the concept of incipient separation of turbulent boundary layers[7] indicates that an airfoil section with an inflection station in the rear may offer special characteristics of limiting the excursion of the center of pressure in general and decreasing the wave drag in a supercritical flow in particular. The hypothesis has been postulated based only on theoretical argument. The concept is completely new and needs to be proven with rigorous theoretical analysis and verified with careful experiment. The present work is the first theoretical step toward the development of a new airfoil.

THEORETICAL CONSIDERATIONS

INVISCID WAVE DRAG

In a transonic supercritical flow, the local supersonic flow must be generally terminated by a shock wave for the flow to return to its subsonic state far downstream. The inviscid shock is characterized by a pressure jump and is associated with an entropy change across the wave. The latter is responsible for the drag rise. Its magnitude can be determined by the following equation:[8]

$$D = V_\infty \int_{\sigma_\infty} \rho V_n \, G(M_\infty, \, s-s_\infty) d\sigma \tag{1}$$

where

$$G(M_\infty, \, s-s_\infty) = 1 - \sqrt{1 + \frac{2}{(\gamma-1)M_\infty^2} \left(1 - e^{\frac{\gamma-1}{\gamma} \frac{s-s_\infty}{R}}\right)} \tag{2}$$

---

[6] Tai, T.C., "Transonic Inviscid Flow over Lifting Airfoils by the Method of Integral Relations," AIAA Journal, Vol. 12, No. 6 (Jun 1974) pp. 798-804.

[7] Tai, T.C., "Optimization of Axisymmetric Thrust Augmenting Ejectors," AIAA Paper No. 77-707, presented at AIAA 10th Fluid & Plasma Dynamics Conference, Albuquerque, N. Mex. (Jun 1977).

[8] Steger, J.L. and B.S. Baldwin, "Shock Waves and Drag in the Numerical Calculation of Isentropic Transonic Flow," NASA TN D-6997 (Oct 1972).

The integration covers the entire shock surface. The quantity V_n is the normal velocity component ahead of the shock wave and $(s-s_\infty)$ is the entropy change across the shock wave.

$$\frac{s-s_\infty}{R} = \ln \left\{ \left[1 + \frac{2\gamma}{\gamma+1} \left(M_1^2 - 1 \right) \right]^{\frac{1}{\gamma-1}} \left[\frac{(\gamma+1)M_1^2}{(\gamma-1)M_1^2+2} \right]^{\frac{-\gamma}{\gamma-1}} \right\} \qquad (3)$$

Although the above equation is not readily integrable without knowledge of the shape of the shock wave, it does give a clear indication that for an inviscid adiabatic flow the entropy change is the sole source of transonic drag rise. The magnitude of entropy change depends on the flow velocity ahead of the shock, M_1. Any attempt to reduce the transonic drag rise, therefore, should be directed to suppressing the local Mach number ahead of the shock: the smaller the Mach number M, the lower the drag D.

The value of local Mach number, on the other hand, has a direct bearing on the circulation, that is, the lift. The way it affects the lift differs from that for the drag, however. In case of lift, the difference in velocity between the upper and lower surfaces of an airfoil is important and the overall lift results from the sum of this difference over the entire surface. While for drag, as indicated in Equations (1) through (3), only the Mach number in front of the shock is of direct concern. Based on this argument, therefore, it is possible to obtain a high lift-to-drag ratio if the flow velocity on the upper surface is kept as high as possible but is allowed to decelerate smoothly before the local supersonic flow terminates. This is one of the basic concepts employed in the derivation of the dromedaryfoil and will be discussed later. The development of the peaky airfoil of Pearcey[1] and supercritical airfoils of Whitcomb[2] are previous examples applying this concept.

DRAG DIVERGENCE AND TRANSONIC BUFFETING

The problem of wave drag is worsened by viscous effects. The boundary layer grows rapidly because of the steep pressure rise at the shock wave.

On the other hand, the shock location will be altered as a consequence of the boundary layer growth that effectively thickens the airfoil. This phenomenon of mutual interference between the shock wave and boundary layer is referred to as the transonic viscous-inviscid interaction problem.

Physically, in the process of transonic viscous-inviscid interaction, there is a communication of positive pressure disturbance from the shock wave upstream through the subsonic portion of the boundary layer, which, in turn, effectively changes the behavior of the boundary layer far ahead of the shock wave.[9,10] A physically significant situation exists where the boundary layer can "feel" the presence of a shock wave downstream, that otherwise would not be possible through the inviscid region where the flow is supersonic. The response to this as exerted by the boundary layer usually causes flow separation if the shock wave is strong. Such a shock-induced boundary layer separation is usually severe enough to produce the well known drag divergence and transonic buffeting problems.

In order to suppress drag divergence and transonic buffeting, more effort is required to reduce the degree of viscous-inviscid interaction by (a) thinning the boundary layer ahead of the shock wave and (b) fixing the shock location. The former has an effect of forcing the boundary layer to become supercritical so that the communication of positive pressure disturbance may be blocked.* The latter eliminates excursion of the shock wave so that the magnitude of disturbance may be minimized. It will be discussed later how these two concepts are implemented in the development of the dromedaryfoil.

As in the other flow regimes, the ultimate concern in airfoil design at transonic speeds is the value of lift-to-drag ratio at design and

---

[9]Klineberg, J.M. and L. Lees, "Theory of Laminar Viscous-Inviscid Interactions in Supersonic Flow," AIAA Journal, Vol. 17 (Dec 1969), pp. 2211-2221.

[10]Tai, T.C., "Transonic Laminar Viscous-Inviscid Interaction over Airfoils," AIAA Journal, Vol. 13, No. 8 (Aug 1975), pp. 1065-1072.

*A thin boundary layer may become supercritical because a large portion of the boundary layer may be actually supersonic since the flow at the edge of the boundary layer is supersonic before the shock wave.

off-design conditions. The drag divergence is usually accompanied by reduction in lift, i.e., the value of lift-to-drag decreases sharply when the drag diverges. One must consider, therefore, the overall lift and drag situation rather than isolating one from the other.

In this regard, the compression after the shock wave plays a dominant role. Theoretically, the higher the lift coefficient, the higher the circulation. The high circulation is generated by a large velocity on the upper surface and thus requires more compression after the shock wave where the flow is subsonic in both inviscid and viscous regions and the boundary layer is de-energized after passing through the severe adverse pressure gradient at the shock. The outer subsonic compression produces a continuous adverse pressure gradient that causes further instability of the boundary layer toward separation.

Such a situation may be improved by (a) reducing the strength of the shock and (b) applying incipient separation criterion toward the trailing edge. The former will eventually stabilize the boundary layer after the shock. The latter keeps the flow at imminent separation condition so that the compression may be accomplished at minimum skin frictions and thus achieve high lift-to-drag values. These concepts are also implemented in the derivation of the dromedaryfoil.

LIMITING SHOCK STRENGTH

The focal point of high supercritical flows is therefore the strength of the shock wave. One might expect that the higher the free-stream Mach number, the higher the local supersonic velocity and thus the stronger the shock wave. This statement is true to the extent of moderate free-stream speed. As the free-stream Mach number further increases, the shock strength will eventually approach a maximum value. The shock strength can be represented by the static pressure behind the shock, which can be found in a standard text.[11]

---

[11] Liepmann, H.W. and A. Roshko, "Elements of Gasdynamics," John Wiley, New York (1957), pp. 53 and 59.

$$\frac{P_2}{P_{0_1}} = \frac{2\gamma M_1^2 - \gamma + 1}{\gamma + 1} \left(1 + \frac{\gamma - 1}{2} M_1^2\right)^{-\frac{\gamma}{\gamma - 1}} \tag{4}$$

Let

$$\frac{d\left(P_2/P_{0_1}\right)}{dM_1} = 0$$

one obtains

$$M_1 = \sqrt{\frac{\gamma + 3}{2}} = 1.483 \text{ (for } \gamma = 1.4) \tag{5}$$

The limiting pressure coefficients at a shock wave is therefore:

$$C_{P_{1im}} = \frac{2}{\gamma M_\infty^2} \left\{ \left[\frac{2 + (\gamma - 1) M_\infty^2}{2 + (\gamma - 1)(\gamma + 3)/2} \right]^{\frac{\gamma}{\gamma - 1}} - 1 \right\} \tag{6}$$

The above result was first found by Laitone[12] and is known as the limiting velocity principle. The result is valid only in front of the shock where Equation (4) holds. A plot of P_2/P_{0_1} versus M_1 is given in Figure 1a which indicates that the minimum pressure after the shock may be as much as 67 percent of the total pressure ahead of the shock. If $M_1 > 1.483$ then P_2/P_{0_1} is less than it would be for $M_1 = 1.483$. The downstream pressure, which is always greater than P_2, can force the shock wave upstream until the location where $P_2/P_{0_1} = 0.67$ is reached. Note that Equation (6) is not valid for the leading edge region where the "peaky" pressure may well exceed the Mach 1.483 value.

The theoretical limiting pressure coefficients given by Equation (6) are presented in Figure 1b along with experimental data obtained by

---

[12]Laitone, E.V., "Limiting Velocity by Momentum Relations for Hydrofoils near the Surface and Airfoil in near Sonic Flow," Proceedings of the 2nd U.S. National Congress of Applied Mechanics (Jun 1954).

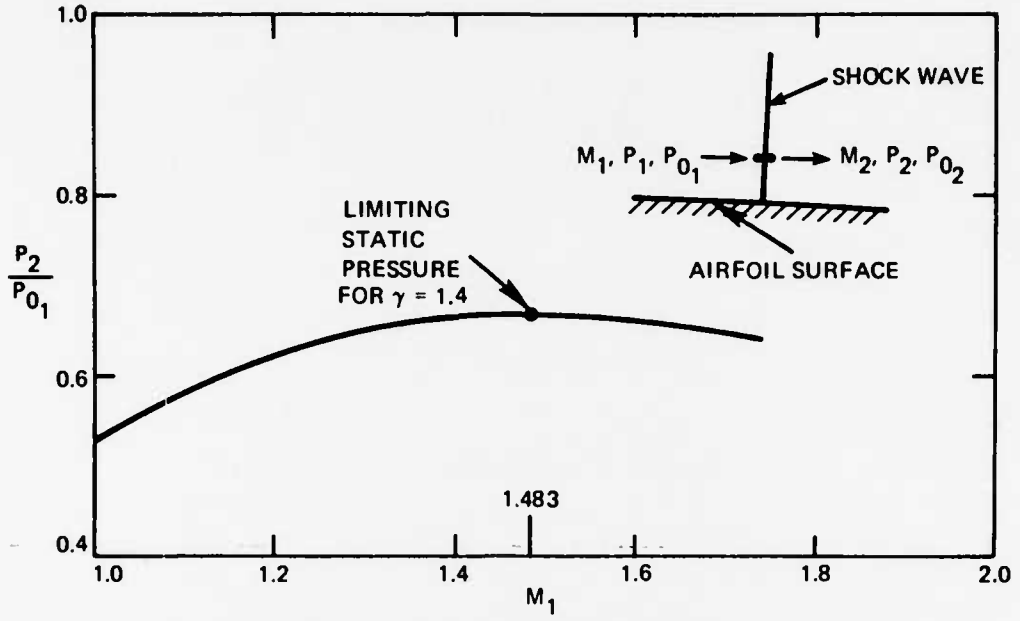

Figure 1a - Static Pressure behind a Normal Shock Wave

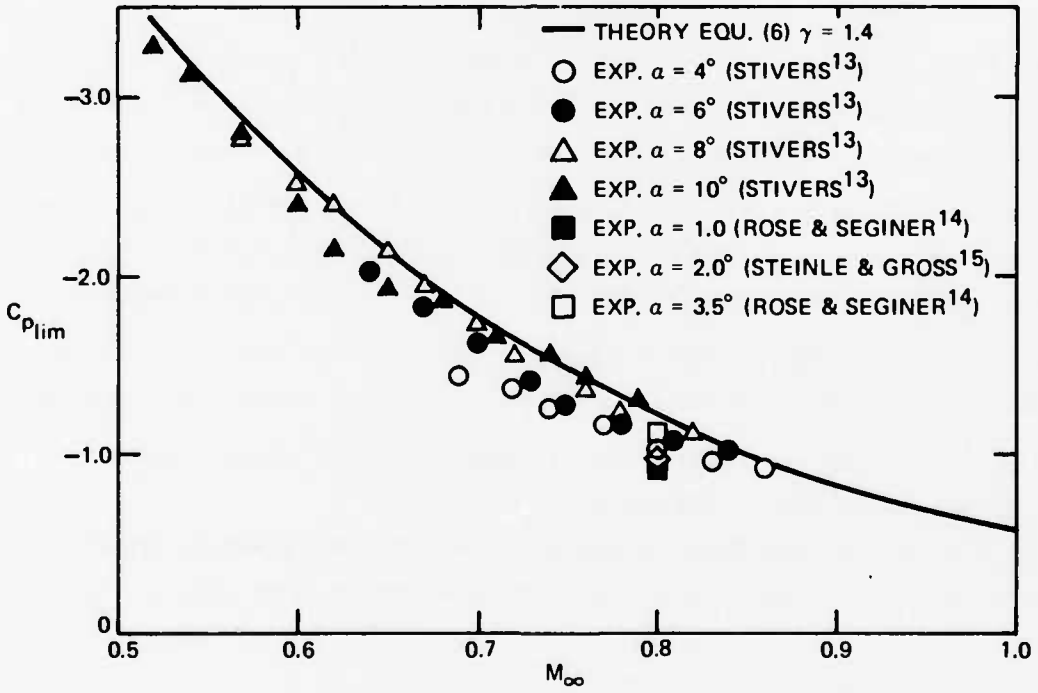

Figure 1b - Limiting Pressure Coefficients at Various Free Stream Conditions

Figure 1 - Limiting Shock Strength at Supercritical Speeds

Stivers,[13] Rose and Seginer,[14] and Steinle and Gross.[15] Stivers' data[13] were based on a 64A410 airfoil, while those of Rose and Seginer[14] were taken on a Yoshihara "A" supercritical airfoil. Steinle and Gross[15] used a 64A010 airfoil. All the data points lie within the theoretical limiting line with $\gamma = 1.4$ for an ideal air except three points of Stivers' 64A410 airfoil at $\alpha = 10$ deg. The reason is that the shock wave moved toward the leading edge region at high angle of attack where Equation (6) becomes less valid as mentioned before. It is observed from the experimental data that for the same airfoil, either 64A410 or 64A010, the higher the angle of attack, the sooner the limiting pressure is reached. The supercritical airfoil offers more leeway toward the limiting boundary; but this may be attributed to its low angle-of-attack setting.

There may be possibilities that multishock waves appear in cases of extreme flow conditions. If that is the case, the strength of the main shock wave should still be governed by Equation (6).

Laitone's limiting velocity principle is readily extended to oblique shock wave cases by considering variations of both Mach number M_1 and shock angle β. In so doing, there results

$$M_1 = \frac{1.483}{\sin \beta} \tag{7}$$

The derivation of Equation (7) is given in the appendix. The above equation indicates that the lower the shock angle β, the higher the local Mach number in extreme flow conditions. Since the strength of the shock

---

[13]Stivers, L.S., Jr., "Effects of Subsonic Mach Numbers on the Forces and Pressure Distributions on Four NACA 64A-Series Airfoil Sections at Angles of Attack as High as 28°," NACA TN3162 (Mar 1954).

[14]Rose, W.C. and A. Seginer, "Calculations of Transonic Flow over Supercritical Airfoil Sections," AIAA Paper No. 77-681, presented at AIAA 10th Fluid and Plasma Dynamics Conference, Albuquerque, N.M. (Jun 1977).

[15]Steinle, F.W., Jr. and A.R. Gross, "Pressure Data from a 64A010 Airfoil at Transonic Speeds in Heavy Gas Media of Ratio of Specific Heats from 167 to 112," NASA TM X-62468 (1975).

wave is determined by the product of M_1 and $\sin\beta$, the ultimate value of the shock strength is therefore fixed and the local Mach number is allowed to exceed the 1.483 limit. In view of this modification, therefore, it will be more appropriate to refer to it as the principle of limiting shock strength.

DERIVATION OF DROMEDARYFOIL

Based on previous considerations, an airfoil that will perform reasonably well at off-design conditions in a high supercritical flow must have the following:

(a) Basic features of a supercritical airfoil, i.e., the chordline almost parallel to free stream, reduced curvature of the midchord region of the upper surface, high pressure recovery for the rear part of the lower surface, and cusp at the trailing edge; and

(b) Various aspects as discussed in the previous section, i.e., isentropic compression ramp ahead of the shock, a sharp corner for fixing the shock location and converting the normal shock to an oblique one, and incipient separation on the rear upper surface after the shock.

The basic new airfoil is, therefore, derived by using a typical existing supercritical airfoil incorporated with a sharp hump for implementing those concepts in (b). The hump has a short curved ramp in the front of the peak and incipient separation surface from the peak leveling off toward the trailing edge. The location of the hump should coincide with a theoretically determined shock location for a typical supercritical flow condition. The new airfoil is named dromedaryfoil* to symbolize the sharp hump. A typical dromedaryfoil is depicted in Figure 2 and the basic difference in shock wave patterns of existing airfoil and dromedaryfoil is schematically presented in Figure 3.

The leading edge of a dromedaryfoil has moderate, but slightly reduced, bluntness as compared with an ordinary supercritical airfoil. The

*The name "dromedaryfoil" was suggested by Dr. S. de los Santos of DTNSRDC.

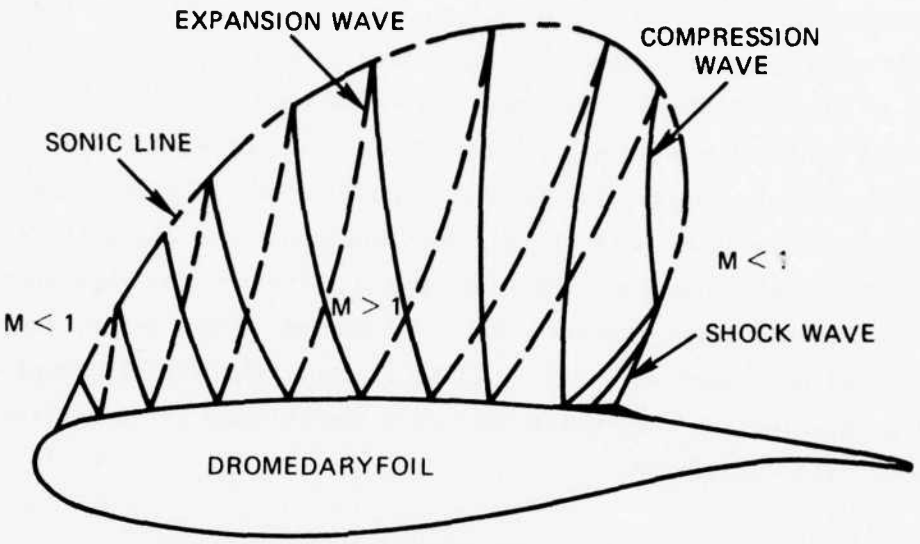

Figure 2 - A Typical Dromedaryfoil

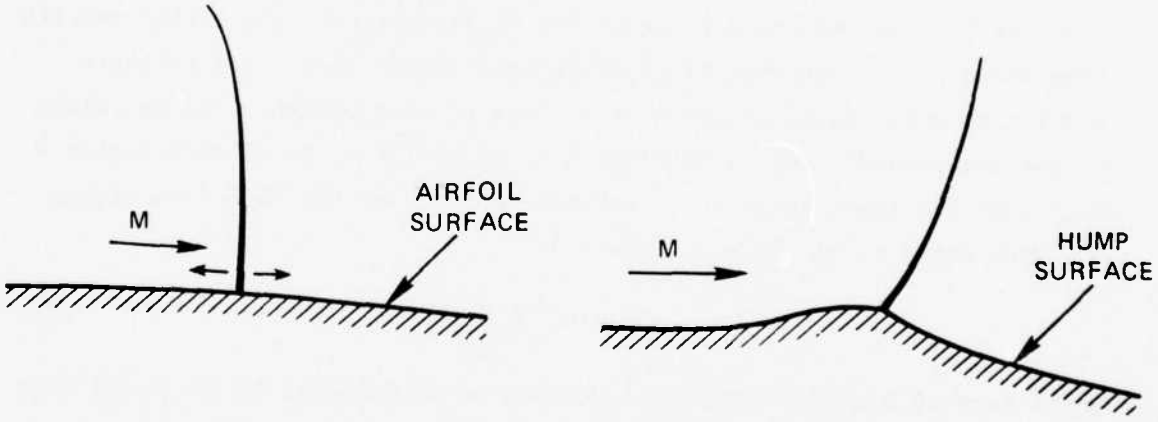

EXISTING AIRFOIL

- SHOCK WAVE MOVES
  - SIGNIFICANT C.P. TRAVEL (BUFFET INDUCED)
- NORMAL SHOCK FOOT
  - $M_{max} = 1.483$

DROMEDARYFOIL

- SHOCK WAVE FIXED
  - C.P. TRAVEL REDUCED (BUFFET SURPRESSED)
- OBLIQUE SHOCK FOOT
  - $(M \sin \beta)_{max} = 1.483$

Figure 3 - Shock Wave Patterns of Existing Airfoil and Dromedaryfoil

inviscid flow mechanism over a dromedaryfoil is characterized by expansion and compression waves over the mildly, curved upper surface. Flow recompression starts from the midchord region and is enhanced near the hump. Because of the presence of the hump, the shock wave will become oblique, instead of a normal one from a pure inviscid point of view. The flow then undergoes subsonic compression from the shock to the trailing edge. Flow recompression initiates near the midchord and continues along the rear surface which satisfies incipient separation criterion for high pressure recovery. On the lower surface, the flow remains in the subcritical state by very mild acceleration in the leading region. The overall shape of the trailing edge forms a cusp which acts as a curved flap for generating much of the airfoil circulation.

GEOMETRY AND CHARACTERISTICS OF THE HUMP

FORE COMPRESSION RAMP

The short curved ramp in front of the hump peak serves as a decelerating zone immediately before the shock wave. Its purpose is to weaken the shock strength so that the wave drag will be reduced according to Equation (1) and the boundary layer may be stabilized. The latter results from the overall reduction of pressure rise rather than local pressure gradients, which would be positive in case of compression. The curvature of the compression ramp is determined by the value of local Mach number M such that the angle between the surface tangent and the Mach line equals the Mach angle μ, as shown in Figure 4:

$$\mu = \sin^{-1}\left(\frac{1}{M_1}\right) \tag{8}$$

The values of μ vary between 42.4 degrees to 90 degrees, if the local Mach number is decelerated from a maximum of 1.483 to an ideal value of unity at the peak. By virtue of the above criteria, the designed shape of ramp surface will be concave in the fore portion, becoming convex near the end.

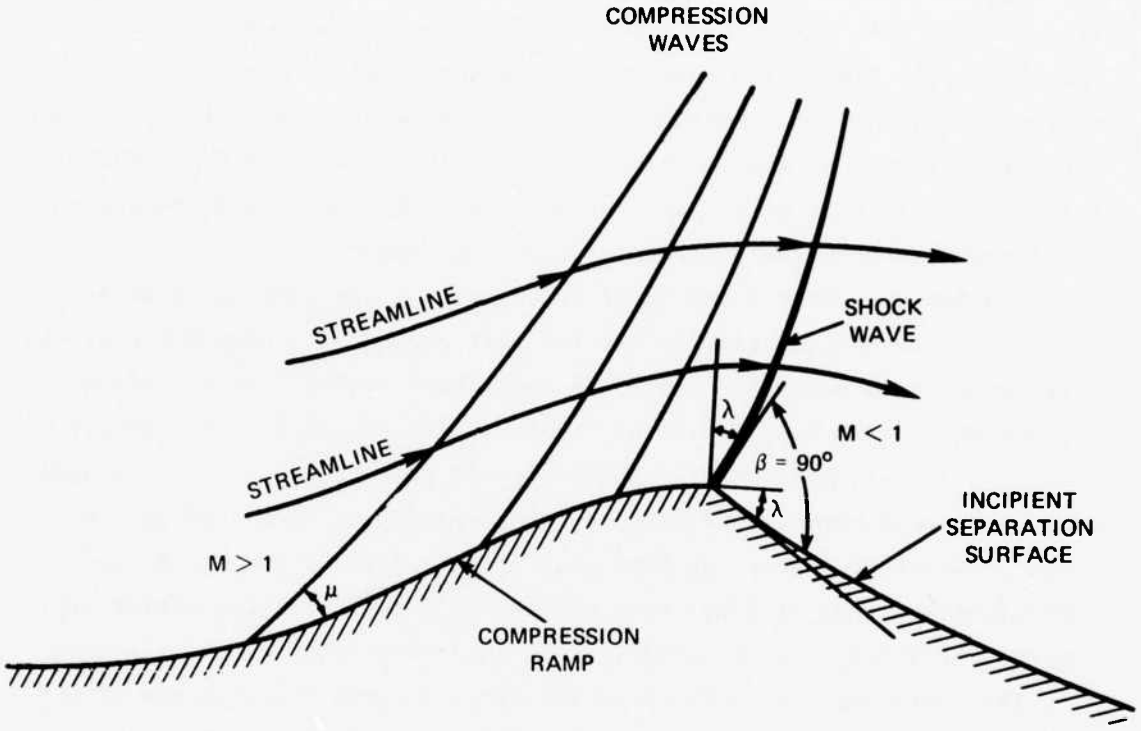

Figure 4 - Geometry of the Hump of a Dromedaryfoil

HUMP PEAK

At the end of compression ramp is the peak of the hump, where the local Mach number will reach unity as the design condition. Because of nonlinearity of the flowfield, when either the free stream Mach number or the angle of attack increases, this ideal value may not be achievable. The flow in turn will have a shock wave at the peak of the hump to terminate the supersonic flow. The strength of the shock wave depends much on the degree of compression accomplished by the compression ramp; i.e., the more the compression, the weaker the shock strength. The shock foot touches the peak of the hump at an angle of 90 degrees measured with respect to the tangent of the rear surface, as discussed later.

A schematic representation of the flow near the peak is shown in Figure 4. The design criteria for the rear part of the hump are that the flow immediately after the shock has unity Mach number, and the airfoil surface behind the hump satisfies the incipient separation requirement. These two requirements greatly depend on the history of the flow as well as on the local geometry of hump surface. First, we will examine the range of shock angles at the hump peak for the design* and off-design conditions and then will evaluate whether or not these angle limits include an inclination that satisfies the incipient separation criterion.

The shock angle is defined as the angle between the tangents of the shock foot and the rear hump surface. The value of the shock angle can therefore be found if we apply the oblique shock relations[10] locally at the peak:

$$M_2^2 \sin^2(\beta-\theta) = \frac{1 + \frac{\gamma-1}{2} M_1^2 \sin^2 \beta}{\gamma M_1^2 \sin^2 \beta - \frac{\gamma-1}{2}} \qquad (9)$$

where β is the shock angle and θ is the surface inclination; both are measured from the direction of the flow deflected by angle λ ahead of

*At the design condition, a sonic line should appear in place of the shock wave.

the shock. At the design condition of $M_1 = 1.0$ and across the sonic line we must have $M_2 = 1.0$, there results

$$\beta = 90 \text{ deg and } \theta = 0 \tag{10}$$

It implies that the shock foot (in this case, the tip of the sonic line) lies at 90 deg measured from the tangent of rear hump surface; see Figure 4.

The flow along the surface streamline eventually experiences a turn of angle λ before the supersonic region is terminated. Away from the surface, however, because of the nonlinear nature of the flow field, such a turn may not necessarily be accompanied by flow expansion.* The streamlines in the flow field are influenced by the presence of the hump, however. The flow is decelerated from supersonic to subsonic speed and then followed by subsonic diffusion downstream of the sonic line.

At the design condition, the angle λ is the only factor that might affect imposing another criterion--the incipient separation condition. However, since λ can be anywhere between 0 and 45 deg as discussed later, the wide range of permissible λ values presents no real constraint for applying the incipient separation condition.

The off-design condition which is limited to $M_1 \sin \beta = 1.483$, as previously determined, the limiting angle for the rear hump surface can be evaluated with the aid of Equation (9) along with the relation between the shock angle β and surface inclination θ.[10]

$$\tan \theta = 2 \cot \beta \frac{M_1^2 \sin^2 \beta - 1}{M_1^2(\gamma + \cos 2\beta) + 2} \tag{11}$$

For the limiting off-design condition of $M_1 \sin \beta = 1.483$, the flow condition immediately aft of the oblique shock foot is governed by

$$M_2^2 \sin^2 (\beta - \theta) = 0.5 \tag{12}$$

and

---

*Nonlinear nature here excludes the Prandtl-Meyer type relation between the flow expansion and the turning angle.

$$\tan \theta = \frac{(\gamma+1) \sin 2\beta}{(\gamma+3)(1.4+\cos 2\beta) + 4 \sin^2\beta} \tag{13}$$

Here we have two equations with three unknowns, namely, β, θ, and M_2. The problem is therefore indeterminate based on the above system. Physically, however, there must be an equilibrium condition under which the shock may be stabilized. To establish such a condition, consider the pressure value after the shock wave:

$$\frac{P_2}{P_{0_2}} = \left(1 + \frac{\gamma-1}{2} M_2^2\right)^{-\frac{\gamma}{\gamma-1}} \tag{14}$$

If the pressure takes on an intermediate value, the downstream pressure which is always higher than the shock value due to subsonic nature, will adjust the shock wave to an angle such that the maximum pressure can be achieved. Examining Equation (14), we see that the M_2 must be minimum. Accordingly, let,

$$\frac{\partial M_2}{\partial \beta} = 0 \tag{15}$$

Utilizing Equations (12) and (15), we get

$$\frac{\partial M_2}{\partial \beta} = \frac{-0.5}{\tan(\beta-\theta) \sin(\beta-\theta)} \tag{16}$$

therefore

$$\tan (\beta-\theta) \to \infty$$

or

$$\beta-\theta = 90 \text{ deg} \tag{17}$$

Values for β and θ that satisfy both Equations (17) and (13) are

$$\beta = 90 \text{ deg}, \ \theta = 0 \tag{18}$$

The results are identical with those at the design condition as given in Equation (10). The above procedure also excludes any possibility of having a supersonic flow behind the shock foot. Substituting Equation (18) into (12) there results $M_2 = 0.707$, which is eventually the same as if the airfoil is plain (without hump) having normal shock with limiting velocity of $M_1 = 1.483$.

For upstream condition with M_1 between 1.0 and 1.483, the shock inclination may be determined in accordance with Equations (9) and (11). The solution gives a range of $(\beta-\theta)$ values varying from 90 to 135 degrees as M_1 increases from 1.0 to 1.483. Since practically the values of $(\beta-\theta)$ are limited to 90 degrees as discussed previously, any angle in excess of this limit would be the angle for flow deflection, i.e., λ. The value of angle λ therefore varies from 0 to 45 degrees. The variation of shock angle at the hump on dromedaryfoils corresponds to the variation of shock location on conventional airfoils, including supercritical ones.

The above treatments are restricted to the shock foot (at the hump surface) only. Away from the surface, the shock is curved and its shape must be determined by a nonlinear solution. For high supercritical flows where the free-stream Mach number or angle of attack is considerably higher than the design value, the above treatment may be considered as a boundary condition at the hump rather than a solution itself. This is extremely important in obtaining an adequate solution by any numerical procedures. A test should be given in those cases to determine if the local Mach number before the shock wave exceeds the 1.483 limit. If a method gives an answer with $M_1 > 1.483$, it implies that the method becomes inadequate at this stage and corrective action must be taken by limiting the local Mach number in front of the shock to 1.483.

REAR INCIPIENT SEPARATION SURFACE

The above considerations imply that practically no constraint will be imposed by the shock wave in determining the rear hump surface in accordance with the incipient separation condition.

The surface is therefore derived with the condition of $M_2 = 1.0$ at the edge of the boundary layer starting from the peak of the hump. The thickness of the boundary layer is assumed thin enough to ignore any influence of the history of boundary layer development. To obtain the surface contour, attention is focused on maximum pressure recovery under the design $M_2 = 1.0$ condition. This is achieved by specifying a pressure gradient at the rear end of the peak high enough to reduce the skin friction value to as low as possible on the surface. The application is based on an argument that the boundary layer can withstand a nearly infinite adverse pressure gradient for a very short distance without separation. After a few steps the pressure distribution is so specified that the turbulent boundary layer remains attached but in a state of imminent separation. This minimum skin friction on the wall is, in principle, equivalent to the incipient separation criterion in the conventional approach such as the one proposed by Stratford.[16] It is eventually an inverse problem which requires an iterative process. Since at the design condition the shock strength has been minimized by the hump, the transonic weak interaction approach has been employed in the present viscous region associated with the turbulent boundary layer. In the iterative process, the rear hump surface is specified in a similar manner as the other part of the airfoil and the inviscid and viscous flows are subsequently calculated. The resulting skin friction values on the rear hump surface are checked to meet the specified values. The rear hump surface is then redefined and the procedure is repeated until specified values of skin friction are met.

NUMERICAL METHODS

Numerical methods are employed to analyze the flow characteristics and to iteratively determine the rear hump surface of the dromedaryfoil. For subcritical flow and low supercritical flows, the computer code developed by Bauer et al.[17] based on potential flow equations solved with the

---

[16] Stratford, B.S., "The Prediction of Separation of the Turbulent Boundary Layer," J. of Fluid Mechanics, Vol. 5 (Jan 1959), pp. 1-16.

[17] Bauer, F. et al., "Supercritical Wing Sections II A Handbook," Lecture Notes in Economics and Mathematical Systems, Vol. 10, Springer-Verlag (1975).

the aid of line relaxation by finite difference scheme has been utilized. The code has the ability for predicting flow characteristics up to M_∞ = 0.75 for a typical airfoil at low angle of attack. The lower the free-stream Mach number, the better the convergence. The method breaks down in cases of high supercritical flows, or airfoil at high angles of attack.

The approach based on full inviscid flow equations using the method of integral relations developed by the present author previously was employed for high free-stream Mach numbers.[6] The condition of limiting shock strength has been incorporated as necessary so that the method is adequate in handling off-design performance analysis. By imposing the limiting shock strength condition of $(M_1 \sin \beta)_{max} = 1.483$, the shock wave will consequently move forward for conventional airfoils. In case of a dromedaryfoil where the shock wave is fixed, the imposition of such a condition implies that the flow has deviated from its normal operation condition.

The application of incipient separation on the rear hump surface was implemented with the aid of the semi-empirical integral approach of Nash and MacDonald.[18] The viscous approach was coupled with the inviscid solution in a weak interaction manner where flow separation did not occur. The procedure is adequate in handling the design condition of the dromedaryfoil for which the shock wave is expected to be weakened by humping.

PRELIMINARY RESULTS AND DISCUSSION

Using a Korn-Garabedian, 16-percent thickness supercritical airfoil (later designated as K-G airfoil) as the base airfoil, four dromedaryfoils have been derived, designated as D-0, D-1, D-2, and D-3. The D-0 dromedaryfoil has coordinates identical with the K-G airfoil except that a sharp hump is mounted at 0.66 c; the rear surface from the hump to the trailing edge does not satisfy the incipient separation criterion either. Dromedaryfoils D-1, D-2, and D-3 are obtained by modifying the leading edge of the K-G airfoil with various hump locations. The reason for the leading

---

[18] Nash, J.F. and A.G.I. MacDonald, "The Calculation of Momentum Thickness in a Turbulent Boundary Layer at Mach Number up to Unity," Aeronautical Research Council, C.P. No. 963 (1967).

edge modification was to reduce the negative lift at high free-stream Mach numbers to counteract the flow due to humping. These airfoils are shown in Figure 5.

Figure 6 shows the pressure distributions along dromedaryfoil D-0 and K-G airfoil at subcritical flow conditions of M_∞ = 0.525 and 0.585, using the computer code by Bauer et al. The flow is accelerated on the forward surface and decelerated on the rear surface of the hump. The trend is correct since the fore ramp has narrowed the flow path which causes the flow to accelerate in the subsonic region. A similar pressure distribution pattern has been observed at both free-stream conditions, which leads to a fairly fixed center of pressure location.

At supercritical flow conditions, the center of pressure excursion is limited in two ways as observed by the pressure distributions along a dromedaryfoil D-3 and a Korn-Garabedian airfoil, as shown in Figure 7. The peak of the hump for the D-3 dromedaryfoil was located at 0.76 c. First, the shock wave appears at the peak of the hump and is followed by a high compression zone toward the trailing edge. For the K-G airfoil, however, the steep pressure jump of the shock appears near the trailing edge. Second, the pressures in the leading edge area also display a different pattern for two foils. By dipping the nose down in dromedaryfoil the negative lift region is considerably smaller than that of the K-G airfoil. Both of the above flow characteristics suggest that the center of pressure remains fairly fixed for the dromedaryfoil but moves toward the trailing edge for the K-G airfoil. Note that these comparisons are made with essentially the same lift and drag coefficients.

The above two figures were concerned with typical subcritical and supercritical flows for two dromedaryfoils. The D-0 dromedaryfoil, which differs from the K-G airfoil by humping only, yields lower wave drag in the moderate speed range but the slope of the drag curve is steeper than that for K-G airfoil when the free-stream Mach number increases, as depicted in Figure 8. Also shown in the figure are wave drag values for D-1, D-2, and D-3 dromedaryfoils. The D-3 dromedaryfoil exhibits a flatter C_{D_w} curve than the K-G airfoil which would perform better in high supercritical flow regions.

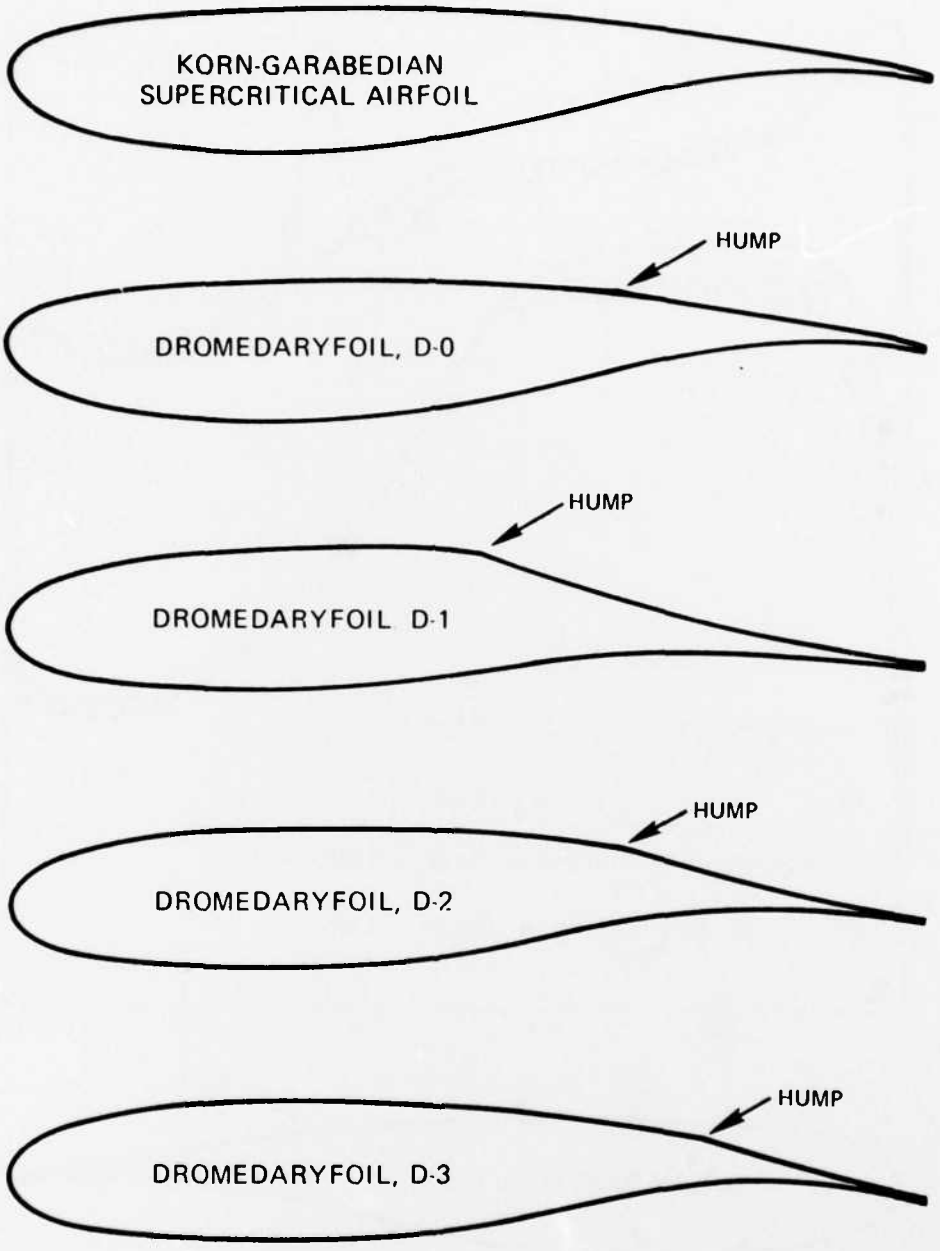

Figure 5 - A Class of Dromedaryfoils along with a Korn-Garabedian Supercritical Airfoil

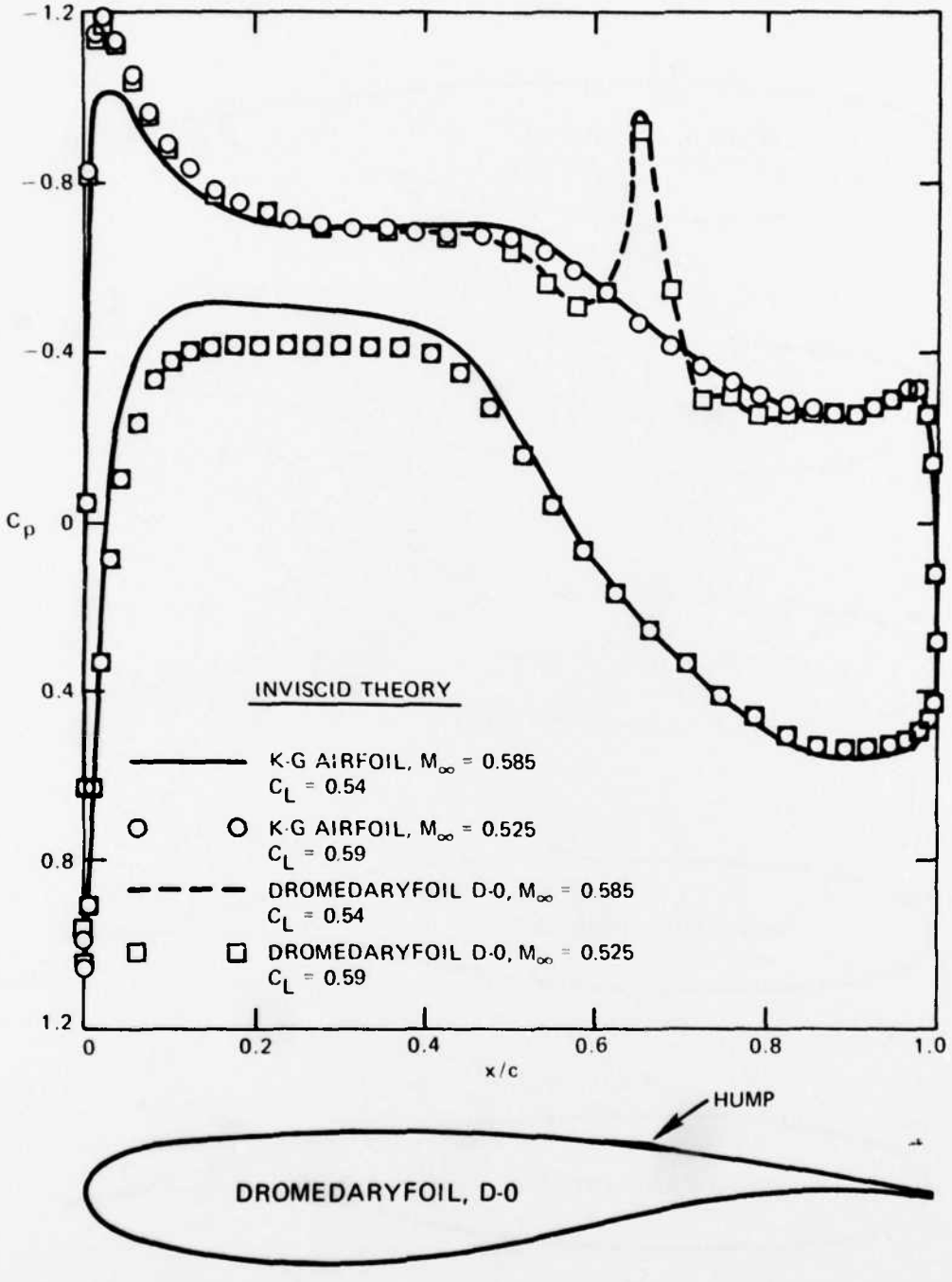

Figure 6 - Theoretical Pressure Distributions on a Dromedaryfoil at Subcritical Speeds

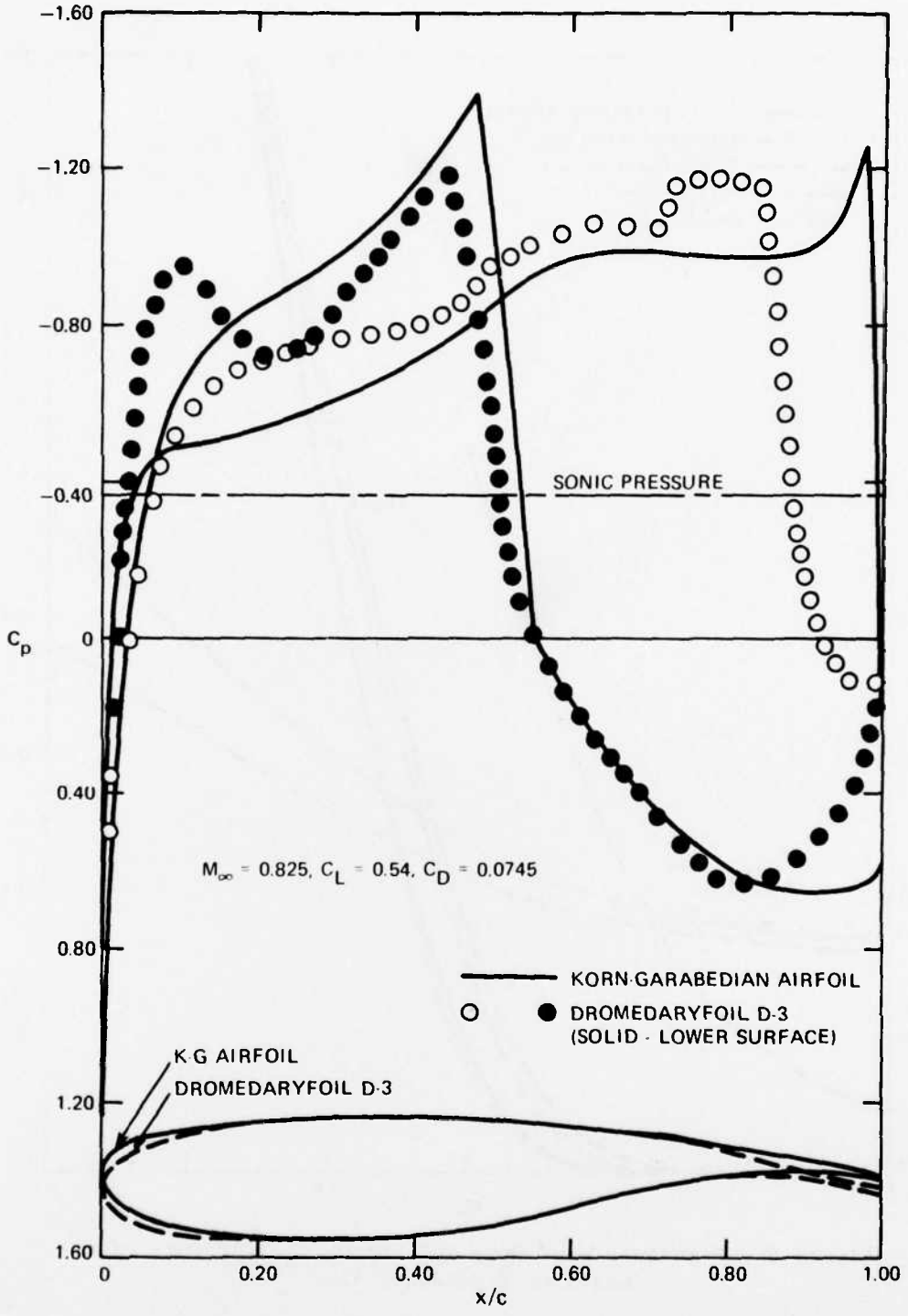

Figure 7 - Theoretical Pressure Distributions on a Dromedaryfoil and a Korn-Garabedian Airfoil at Supercritical Speeds

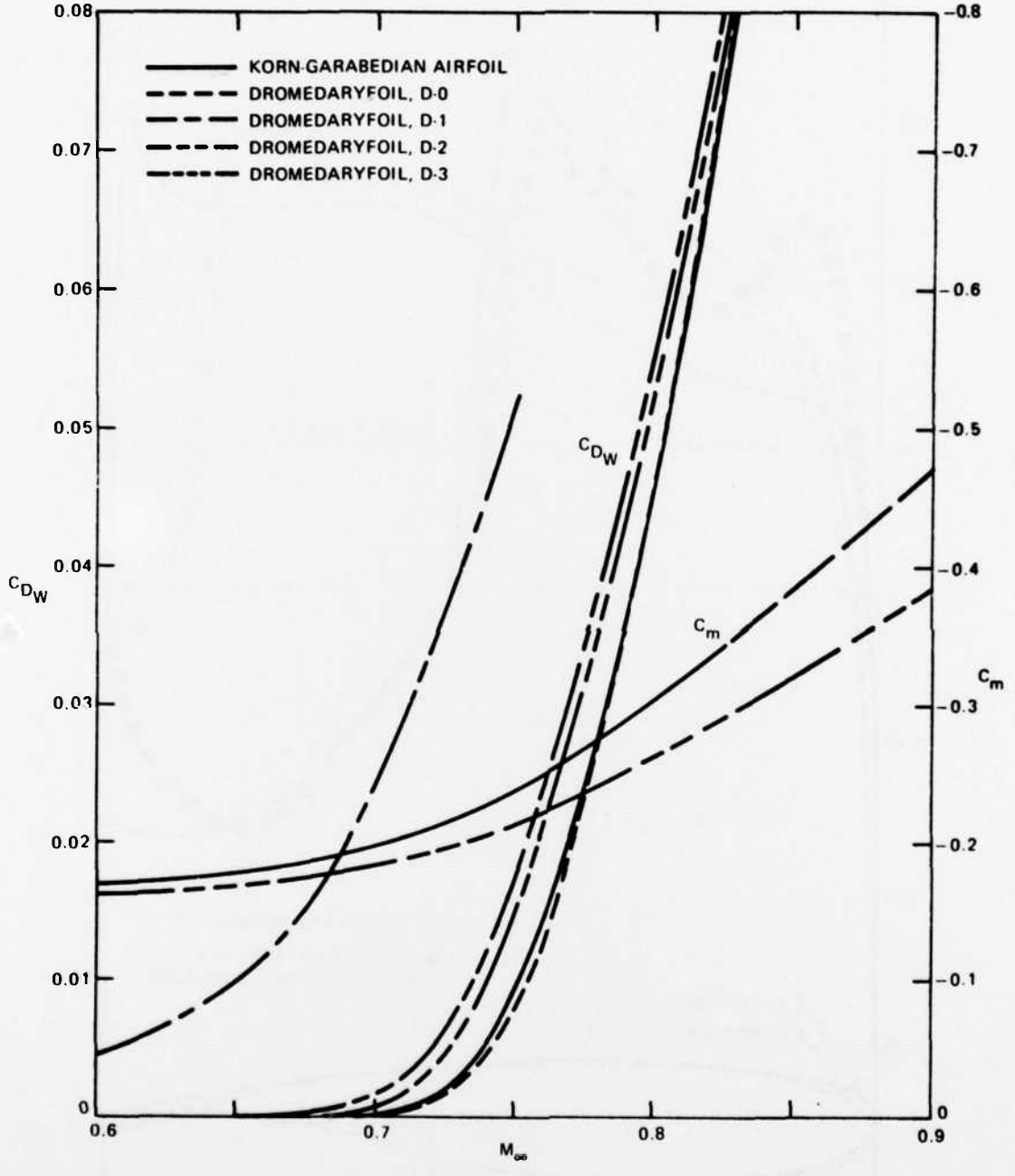

Figure 8 - Transonic Wave Drag and Moment Coefficients of a Class of Dromedaryfoils

The drag curves for D-1 and D-2 indicate fairly higher drag values than the original supercritical airfoil. It implies that improper humping would be penalized by increased wave drag in most speed regions. Simple humping* could be as bad as improper humping,* as in the case of the D-0 dromedaryfoil in the high speed region.

Comparison of the pitching moment coefficient (C_m) curves in Figure 8 indicates the rate of increase in C_m being considerably smaller for the dromedaryfoil than for the supercritical airfoil. Since the pitching moment has a direct bearing on the location of the center of pressure, a smaller rate of increase in C_m means slower movement of center of pressure (C.P.) toward the trailing edge. The trend is explicitly demonstrated in Figure 9 where the center of pressure location is plotted against the free-stream Mach number. As the M_∞ increases from 0.70 to 0.86, the center of pressure moves downstream by 0.38 c for the supercritical airfoil, but only 0.27 c for the D-3 dromedaryfoil. In the former the C.P. already reached the trailing edge while in the latter, the C.P. travels only to 0.86 c. Again, the above C_m and C.P. results are based on the same lift and drag coefficients for both cases.

CONCLUDING REMARKS AND RECOMMENDATIONS

The development of the dromedaryfoil concept so far has been based on theoretical considerations only. The results are regarded inconclusive without experimental verification. From theoretical work, some concluding remarks can be drawn:

1. Proper humping of an airfoil with a sharp corner leads to fixed shock wave which limits the excursion of the center of pressure. However, improper humping would be penalized by increased wave drag.

2. With a sharp hump, the shock foot will be inclined at an angle between 0 to 45 deg measured from the flow direction ahead of the shock at the peak of the hump.

---

*By simple humping we mean that a dromedaryfoil is derived by simply mounting a hump on an existing airfoil without any modification to other parts of the airfoil; while improper humping means that a dromedaryfoil is designed improperly without considering overall performance of the airfoil.

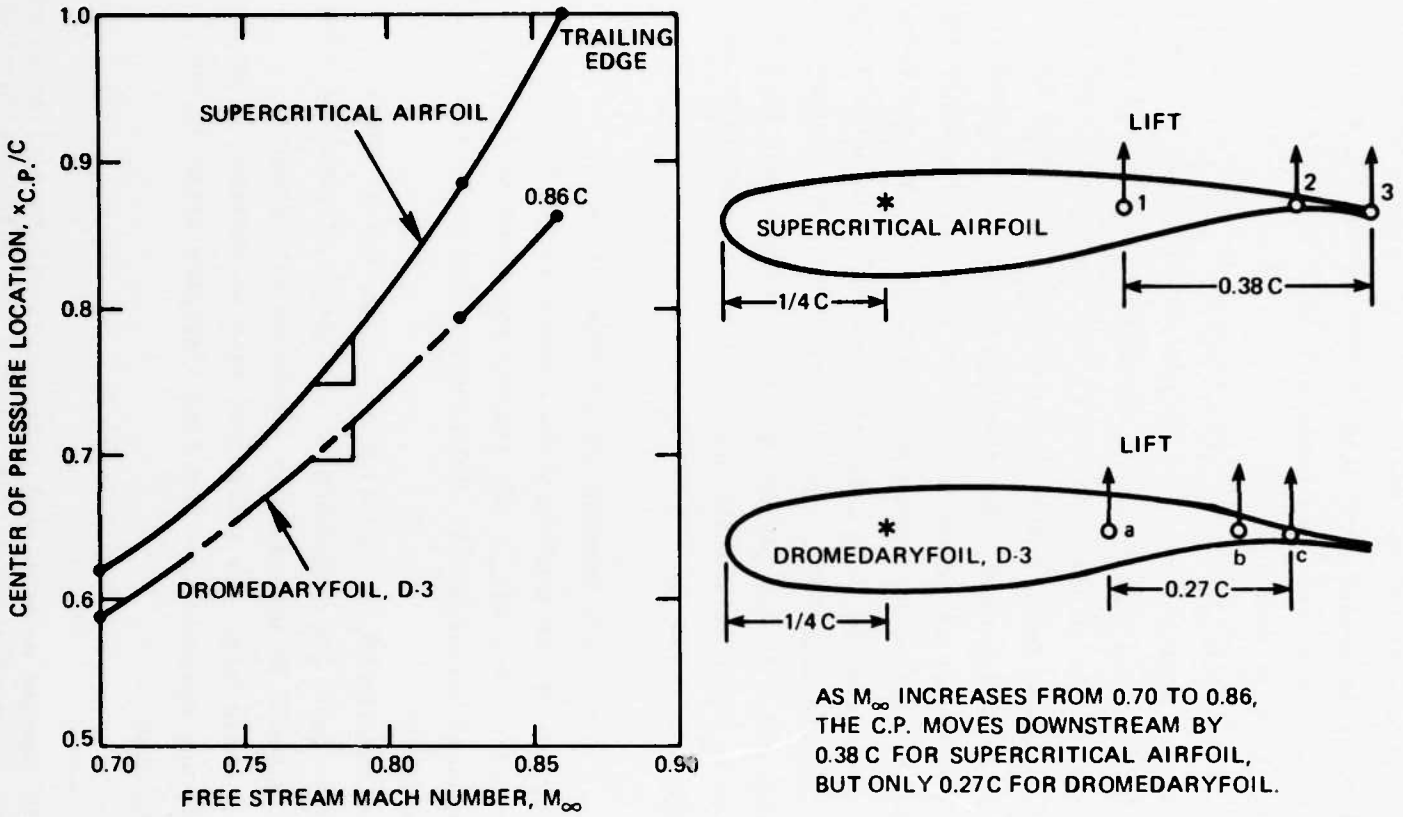

Figure 9 - Change in Center of Pressure on Airfoils at Supercritical Speeds

3. At high supercritical flows, the shock strength would be limited by $(M_1 \sin \beta)_{max} = 1.483$.

4. The transonic drag divergence Mach number may be increased by suppression of shock wave-boundary layer interaction by means of humping and imposing incipient separation on the rear upper surface.

Future investigations recommended:

1. Experimental verification by wind tunnel testing in high Reynolds numbers.

2. Refinements in theoretical design procedures by considering a more sophisticated viscous solution in obtaining the incipient separation surface behind the sharp hump.

3. Optimization of the dromedaryfoil for various mission purposes.

APPENDIX

DERIVATION OF LIMITING SHOCK STRENGTH FOR AN OBLIQUE SHOCK WAVE

The static pressure behind an oblique shock wave, with a shock angle β, is determined by the oblique shock relation:[10]

$$\frac{P_2}{P_{0_1}} = \frac{2\gamma(M_1 \sin\beta)^2 - \gamma+1}{\gamma+1} \left(1 + \frac{\gamma-1}{2} M_1^2 \sin^2\beta\right)^{-\frac{\gamma}{\gamma-1}} \qquad (A.1)$$

where the subscripts 1 and 2 represent conditions before and after the shock wave. The limiting shock strength is determined by minimizing P_2/P_{0_1}. Let

$$\frac{P_2}{P_{0_1}} = F(M_1, \beta) \qquad (A.2)$$

Here F is a function of M_1 and β.

Differentiating Equation (A.1) with respect to M_1 and β, we obtain:

$$\frac{\partial F}{\partial M_1} = \left(1 + \frac{\gamma-1}{2} M_1^2 \sin\beta\right)^{\cdot\cdot \frac{\gamma}{\gamma-1}} \left(\gamma M_1 \sin^2\beta\right) \times$$

$$\left[\frac{4}{\gamma+1} - \frac{2\gamma M_1^2 \sin^2\beta - \gamma+1}{\gamma+1} \Big/ \left(1 + \frac{\gamma-1}{2} M_1^2 \sin^2\beta\right)\right] \qquad (A.3)$$

and

$$\frac{\partial F}{\partial \beta} = \left(1 + \frac{\gamma-1}{2} M_1^2 \sin^2\beta\right)^{-\frac{\gamma}{\gamma-1}} \left(\gamma M_1^2 \sin\beta \cos\beta\right) \times$$

$$\left[\frac{4}{\gamma+1} - \frac{2\gamma M_1^2 \sin^2\beta - \gamma+1}{\gamma+1} \Big/ \left(1 + \frac{\gamma-1}{2} M_1^2 \sin^2\beta\right)\right] \qquad (A.4)$$

Examination of Equations (A.3) and (A.4) reveals that the maximum of F is achieved by letting, $\partial F/\partial M_1 = \partial F/\partial \beta = 0$, i.e.,

$$\frac{4}{\gamma-1} - \frac{2\gamma M_1^2 \sin^2 \beta - \gamma+1}{\gamma+1} \Bigg/ \left(1 + \frac{\gamma-1}{2} M_1^2 \sin^2 \beta\right) = 0 \qquad \text{(A.5)}$$

Simplifying, we get

$$M_1 \sin \beta = \sqrt{\frac{3+\gamma}{2}}$$

$$= 1.483 \text{ for } \gamma = 1.4 \qquad \text{(A.6)}$$

REFERENCES

1. Pearcey, H.H., "The Aerodynamic Design of Section Shapes for Swept Wings," Advances in Aeronautical Sciences, Vol. 3, Pergamon Press, New York (1961), pp. 277-322.

2. Whitcomb, R.T., "Basic Results of a Wind-Tunnel Investigation of an Integral (Unslotted) Supercritical Airfoil Section," Langley Working Paper LWP-505 (Nov 1967); Declassified (Apr 1974).

3. Yoshihara, H. et al., "Lift Augmentation on Planar Airfoils in the Transonic Regime--A High Reynolds Number Wind Tunnel Study," Convair Aerospace Division of General Dynamics, Report CASD-NSC-73-001, San Diego, Calif. (Sep 1973).

4. Nieuwland, G.Y., "Transonic Potential Flow around a Family of Quasi-Elliptical Aerofoil Sections," National Aerospace Laboratory, Amsterdam, The Netherlands, TR T-122 (Jul 1967).

5. Garabedian, P.R. and D.G. Korn, "Numerical Design of Transonic Airfoils," Numerical Solution of Partial Differential Equations, Vol. 2, Academic Press, New York (1971), pp. 253-271.

6. Tai, T.C., "Transonic Inviscid Flow over Lifting Airfoils by the Method of Integral Relations," AIAA Journal, Vol. 12, No. 6 (Jun 1974) pp. 798-804.

7. Tai, T.C., "Optimization of Axisymmetric Thrust Augmenting Ejectors," AIAA Paper No. 77-707, presented at AIAA 10th Fluid & Plasma Dynamics Conference, Albuquerque, N. Mex. (Jun 1977).

8. Steger, J.L. and B.S. Baldwin, "Shock Waves and Drag in the Numerical Calculation of Isentropic Transonic Flow," NASA TN D-6997 (Oct 1972).

9. Klineberg, J.M. and L. Lees, "Theory of Laminar Viscous-Inviscid Interactions in Supersonic Flow," AIAA Journal, Vol. 17 (Dec 1969), pp. 2211-2221.

10. Tai, T.C., "Transonic Laminar Viscous-Inviscid Interaction over Airfoils," AIAA Journal, Vol. 13, No. 8 (Aug 1975), pp. 1065-1072.

11. Liepmann, H.W. and A. Roshko, "Elements of Gasdynamics," John Wiley, New York (1957), pp. 53 and 59.

12. Laitone, E.V., "Limiting Velocity by Momentum Relations for Hydrofoils near the Surface and Airfoil in near Sonic Flow," Proceedings of the 2nd U.S. National Congress of Applied Mechanics (Jun 1954).

13. Stivers, L.S., Jr., "Effects of Subsonic Mach Numbers on the Forces and Pressure Distributions on Four NACA 64A-Series Airfoil Sections at Angles of Attack as High as 28°," NACA TN3162 (Mar 1954).

14. Rose, W.C. and A. Seginer, "Calculation of Transonic Flow over Supercritical Airfoil Sections," AIAA Paper No. 77-681, presented at AIAA 10th Fluid and Plasma Dynamics Conference, Albuquerque, N.M. (Jun 1977).

15. Steinle, F.W., Jr. and A.R. Gross, "Pressure Data from a 64A010 Airfoil at Transonic Speeds in Heavy Gas Media of Ratio of Specific Heats from 167 to 112," NASA TM X-62468 (1975).

16. Stratford, B.S., "The Prediction of Separation of the Turbulent Boundary Layer," J. of Fluid Mechanics, Vol. 5 (Jan 1959), pp. 1-16.

17. Bauer, F. et al., "Supercritical Wing Sections II A Handbook," Lecture Notes in Economics and Mathematical Systems, Vol. 10, Springer-Verlag (1975).

18. Nash, J.F. and A.G.I. MacDonald, "The Calculation of Momentum Thickness in a Turbulent Boundary Layer at Mach Number up to Unity," Aeronautical Research Council, C.P. No. 963 (1967).

INITIAL DISTRIBUTION

Copies	
1	Chief of R&D (ABMDA)
1	U.S. Army Missile Command
4	CHONR 1 211 1 430B 1 432 1 438
1	NRL
4	ONR 1 Boston 1 Chicago 1 London, England 1 Pasadena
1	USNA
1	USNPGSCOL
1	NADC
1	NWC/China Lake
1	NSWC/Dahlgren
1	NSWC/White Oak
11	NAVAIRSYSCOM 1 AIR 03A 1 AIR 03C 1 AIR 310 3 AIR 320 1 AIR 5108 4 AIR 5301
1	NAVSEASYSCOM
12	DDC
1	AFOSR
1	USAFA
1	AF INST TECH

Copies	
1	AEDC
4	NASA 1 HQ, Washington, D.C. 1 Ames Research Center/Lib 1 Langley Research Center 1 Lewis Research Center
1	National Sci Foundation
1	Argonne National Lab T.C. Chawla
1	U of Arkon/Lib
1	Brown U/Div of Engr
2	Calif Inst of Tech 1 Grad Aero Labs 1 Dr. T. Kubota
1	Calif Inst of Tech/Jet Prop Lab
2	U of Calif/Berkeley 1 Prof. M. Holt/Div Aero Sciences 1 Lib
1	U of Calif/L.A.
1	U of Calif/LaJolla
1	U of S Calif/Lib
1	Catholic U of America/Lib
1	U of Cincinnati/ Aerospace Engr
2	Clemson U 1 Dr. T. Yang/Mech Engr Dept 1 Lib
1	Cornell U/Lib
1	Georgia Inst Tech/Lib

Copies	
1	Harvard U/Gordon McKay Lib
1	Johns Hopkins U/Lib
1	U of Illinois/Lib
2	U of Maryland 1 Aerospace Engr 1 Lib
1	MIT/Lib
2	U of Michigan 1 Aerospace Engr 1 Lib
2	New York U/Courant Inst Math Sci 1 Dr. P.R. Garabedian 1 Dr. A. Jameson
1	U of N Carolina/Lib
2	N Carolina State U/Raleigh 1 Dr. F.R. DeJarnette/Mech & Aerospace Engr Dept 1 Lib
1	Pennsylvania State U/Lib
1	Princeton U/Lib
1	Purdue U/Lib
1	Stanford U/Lib
2	U of Tennessee Space In 1 Dr. J.M. Wu 1 Lib
1	U of Virginia/Alderman Lib
2	Virginia Polytech Inst 1 Carol M. Newman Lib 1 Aero & Ocean Engr

Copies	
1	U of Washington/Lib
1	W Virginia U/Dept Aero Engr
1	American Inst of Aeronautics & Astronautics
1	ARO Inc/Lib
1	Bell Aerospace
1	Boeing Company/Seattle
1	Calspan Corp/Buffalo
1	Flow Research/Kent Washington
1	General Dynamics Convair/Lib
1	Grumman Aerospace Corp/Lib
1	Inst for Defense Analyses
1	Lockheed-Georgia Co/Lib
1	Lockheed Missiles & Space Co/Lib
1	LTV Aerospace Corp/Lib
1	McDonnell Douglas St. Louis/Lib
1	Douglas Aircraft Co/Lib
1	Nielson Engr & Res Inc
1	Rockwell International Corp/Lib
1	Northrop Corporate Labs/Lib
1	TRW Systems Group/Lib

CENTER DISTRIBUTION

Copies	Code	
30	5214.1	Reports Distribution
1	522.1	Library (C)
1	522.2	Library (A)
2	522.3	Aerodynamics Lib


MEI
7